Molecular Immunology 48 (2011) 1397–1407

Contents lists available at ScienceDirect

Molecular Immunology

journal homepage: www.elsevier.com/locate/molimm

Tumor necrosis factor alpha pathways develops liver apoptosis in type 1 diabetes mellitus

Paola I. Ingaramo[a], María T. Ronco[a], Daniel E.A. Francés[a], Juan A. Monti[a], Gerardo B. Pisani[b], María P. Ceballos[a], Mónica Galleano[c], María C. Carrillo[a], Cristina E. Carnovale[a,*]

[a] Institute of Experimental Physiology (CONICET), Faculty of Biochemical and Pharmaceutical Sciences (National University of Rosario), Rosario, Argentina
[b] Morphology Area, Faculty of Biochemical and Pharmaceutical Sciences (National University of Rosario), Rosario, Argentina
[c] Physical Chemistry-PRALIB, School of Pharmacy and Biochemistry, University of Buenos Aires, Buenos Aires, Argentina

ARTICLE INFO

Article history:
Received 21 January 2011
Received in revised form 15 March 2011
Accepted 18 March 2011
Available online 9 April 2011

Keywords:
TNF-α
Caspase-8
NFκB
iNOS
JNK
Insulin
Caspase-3
Apoptosis
Liver
Diabetes

ABSTRACT

We analyzed the contribution of TNF-α intracellular pathway in the development of apoptosis in the liver of streptozotocin-induced diabetic rats. In liver tissue, diabetes promoted a significant increase of TNF-α/TNF-R1, and led to the activation of caspase-8, of nuclear factor kappa B (NFκB), and JNK signaling pathways. The activation of NFκB led to an induction of iNOS and consequent increase in NO production. As a consequence of such changes a significant increase of caspase-3 activity and of apoptotic index were observed in the liver of diabetic animals. Importantly, the treatment in vivo of diabetic rats with etanercept (TNF-α blocking antibody) or aminoguanidine (selective iNOS inhibitor) significantly attenuated the induction of apoptosis by reduction of caspase-3 activity. Overall, we demonstrated that in the diabetes enhances TNF-α in the liver, which may be a fundamental key leading to apoptotic cell death, through activation of caspase-8, NFκB and JNK pathways.

1. Introduction

In a relatively short time, hepatic injury has been recognized as a major complication of diabetes mellitus (DM) (Harrison, 2006). Type 1 diabetes is associated with increased risk of chronic liver injury (Kim et al., 2009).

Currently, type 1 DM is considered as an inflammatory process (Alexandraki et al., 2008) in which a significant increase of cytokines IL-6, IL-18, IL-1 and TNF-α was found in the blood of patients with this disease (Esposito et al., 2002; Foss et al., 2007). Hepatocytes are capable to respond to pro-inflammatory cytokines promoting the expression of genes that mediate the inflammatory response (Martin-Sanz et al., 2002). One of the major cytokines released is TNF-α, which can interact with tumor necrosis factor receptor 1 (TNF-R1) and thus can either promote nuclear factor-κB (NFκB) activation or initiate the caspases activation pathway, which plays a major role in execution of apoptosis (Budihardjo et al., 1999). In addition, TNF-α induced signaling from TNF-R1 leads to the activation of different mitogen-activated protein kinase (MAPK) cascades, which ultimately results in the activation of p38 MAPK, extracellular regulated kinase (ERK) and c-Jun activating kinase (JNK) (Wullaert et al., 2006).

NFκB strongly induces the inducible nitric oxide synthase (iNOS or NOS2) gene expression, responsible for the large amounts of nitric oxide (NO) generated in the liver (Rosa et al., 2008). NO is a molecule with a single unpaired electron; it is a highly diffusible free radical that posses both anti-inflammatory and pro-inflammatory activities, depending on its concentration and the tissue where it is produced (Stichtenoth and Frolich, 1998). When NO is present in relatively high concentrations, pathophysiological and indirect effects predominate due to interactions of NO with O_2 or the free radical superoxide (Davis et al., 2001; Stichtenoth and Frolich, 1998). Numerous reports based on studies in rat liver and human cells suggest that NO has the ability to initiate apoptosis (Kolb, 2000; Ronco et al., 2004) evidenced by chromatin condensa-

Abbreviations: DM, diabetes mellitus; STZ, streptozotocin; AG, aminoguanidine; SID, streptozotocin-induced diabetes; ALT, alanine aminotransferase; AST, aspartate aminotransferase.

* Corresponding author at: Institute of Experimental Physiology (CONICET), Faculty of Biochemical and Pharmaceutical Sciences (National University of Rosario), Suipacha 570, 2000-Rosario, Argentina. Fax: +54 341 4399473.
E-mail address: ccarnova@fbioyf.unr.edu.ar (C.E. Carnovale).

0161-5890/$ – see front matter © 2011 Elsevier Ltd. All rights reserved.
doi:10.1016/j.molimm.2011.03.015

tion and DNA fragmentation (Brune et al., 1999). In neonatal mouse cardiomyocytes it has been shown that expression of caspase genes can be regulated in response to NO and that its differential expression could be responsible for the dual role of NO in either promoting or inhibiting cell death. Moreover, an induction of caspase-8 gene expression by NO would be previous to an increase in cell death (Rabkin and Klassen, 2007). Caspase-8 is a member of the cysteine proteases, which is implicated in the apoptotic process and is also required for apoptosis induced by death receptors like TNF-R1 (Kruidering and Evan, 2000). The role of NO in caspase-8 induction was also described in renal tubular epithelial cells and lung endothelial cells (Du et al., 2006; Li et al., 2007).

In this connection, evidence exists that hyperglycemia leads to activation of NFκB, which can mediate endothelial cell apoptosis (Dandona et al., 2007; Ho et al., 2006). Moreover, many researchers have reported an increase in iNOS levels in liver, kidneys and lung of diabetic rats (Haidara et al., 2009; Stadler et al., 2003), while other studies suggest a decrease in NO production or release from endothelial cells and from heart of rats (Traub and Van, 1995; Stockklauser-Farber et al., 2000). The dual behaviour found in different tissues shows that the response to stimuli like hyperglycemia or diabetes depends on the cellular type involved.

The present study was designed to explore the contribution of TNF-α intracellular pathway in the development of apoptosis in the liver in diabetes type 1. In this paper, we demonstrated that during STZ-mediated diabetic liver injury elevated TNF-α interacted with its receptor TNF-R1 and induced activation of caspase-8, NFκB, and JNK signaling pathways. The NFκB activation resulted in an induction of iNOS and the consistent increase in NO production. Owing to such changes a significant increase of apoptosis was consistently observed in the liver of diabetic animals. The final goal of this study was to evaluate if the in vivo treatment with anti-TNF-α, or aminoguanidine, a selective inhibitor of iNOS, can modulate the cell death pathway induced by the diabetic state.

2. Materials and methods

2.1. Animals and surgical procedures

Male Wistar rats weighing 300–360 g were housed in constant temperature rooms and maintained with light/dark intervals of 12 h duration and were fed ad libitum with a standard diet and water. Animals received humane care according to criteria outlined in the "Guide for the Care and Use of Laboratory Animals", National Research Council, Washington D.C.: National Academy Press, 1996. All the experimental protocols were performed according to the Regulation for the Care and Use of Laboratory Animals (Expedient 6109/012 E.C. Resolution 267/02) and approved by the Institutional Animal Use Committee of the National University of Rosario, Argentina.

2.1.1. Treatment of the animals

Streptozotocin-induced diabetes (SID) was induced by a single dose of streptozotocin (STZ) (60 mg/kg body weight, i.p., in 50 mM citrate buffer, pH 4.5). Control rats were injected with vehicle alone. Fifteen days after STZ injection, a time when the toxic effect of the drug on the liver has disappeared (Carnovale and Rodriguez Garay, 1984; Carnovale et al., 1986), serum glucose levels were tested by means of the glucose oxidase method (Wiener Lab., Rosario, Argentina) in samples of diabetic and control animals. The animals were randomized into three groups. Control group, injected with the vehicle citrate buffer only (i.p.) (C); diabetic group, injected with streptozotocin (i.p.) (SID). Insulin treated, diabetic group, on day 15 post-STZ treatment, SID rats received 30 U of insulin (Betasint insulin, BETA S.A laboratories, Argentina) subcutaneously (sc) twice a day (at 8:00 A.M. and 8:00 P.M.) for 15 days (SID + I). Blood glucose levels were measured every day, each time just before insulin injection. Blood samples were obtained from the tail vein and glucose concentrations were measured by means of a Surestep glucometer (Glucostix, Bayer HealthCare, Argentina). Successful induction of diabetes was defined as a blood glucose level of >13.2 mmol/l. The doses of insulin were adjusted to reach target blood glucose levels of 6–9 mmol/l. Between 10 and 12 A.M. on day 30, rats were weighed, anesthetized with sodium pentobarbital solution (50 mg/kg body weight, i.p.) and euthanized. Blood was obtained by cardiac puncture and plasma was separated by centrifugation. Livers were promptly removed and hepatic tissue was either processed for immunohistochemical studies or frozen in liquid nitrogen and stored at −70 °C until analytical assays were performed.

2.1.2. Inhibition of nitric oxide synthesis

For inhibition studies of NO production, after 15 days of diabetes, a group of rats were separated into different groups and received injections of the preferential inhibitor of iNOS enzyme, aminoguanidine (AG). The groups were as follows: Control group, injected with the vehicle citrate buffer only, and receiving AG in isotonic saline i.p. (100 mg/kg body weight) once a day, beginning 3 days before euthanized (Control + AG) (Carnovale et al., 2000); diabetic group receiving AG i.p. (100 mg/kg body weight) once a day, beginning 3 days before euthanized (SID + AG). The whole study lasted one month. Six animals from each group (Control + AG and SID + AG) were euthanatized and the samples were promptly processed.

2.1.3. Inhibition of TNF-α production

A group of rats received ENBREL® (etanercept), a dimeric fusion protein that binds to TNF-α and decreases its role in disorders mediated by excess of TNF-α. Etanercept mimics the inhibitory effects of naturally occurring soluble TNF-α receptors but has a greatly extended half-life in the bloodstream, and therefore a more profound and long-lasting biologic effect than a naturally occurring soluble TNF-R1 (Madhusudan et al., 2005). Etanercept was administered to 6 rats from each group (Control-a-TNF-α and SID-a-TNF-α) in a dose of 8 mg/kg b.w./day twice a week for 15 days.

2.2. Analytical assays

2.2.1. Western blot analysis: iNOS, TNF-α, TNF-R1, p-JNK, activated caspase-8 and t-Bid

For iNOS, TNF-R1, p-JNK and caspase-8 active subunit (p18) detection, liver tissue lysates were prepared by homogenization in 3 volumes of lysating RIPA buffer containing PBS, 1% Triton X-100, 0.5% sodium deoxycholate, 0.1% SDS, 1 mM phenylmethylsulfonyl fluoride, 10 μg/ml leupeptin, and 1 μg/ml aprotinin. After a 30-min-incubation at 0 °C and three freeze–thaw cycles, lysates were cleared by centrifugation at 15,000 rpm for 30 min, and supernatants were kept at −70 °C. For the preparation of mitochondria-enriched fractions, liver tissues were homogenized in 4 volumes of 300 mmol/l sucrose with protease inhibitors. Homogenates were centrifuged at 1000 × *g* to remove unbroken cells, nuclei and heavy membranes. Mitochondria-enriched fractions were then obtained by centrifugation at 3000 × *g* for 15 min at 4 °C (Ronco et al., 2004). Proteins were quantified according to Lowry et al. (1951). For iNOS analysis, 30 μg of protein was subjected to 8% SDS-polyacrylamide gel electrophoresis and transferred to polyvinyl difluoride membranes (PVDF) (PerkinElmer Life Sciences, Boston, MA, USA). For TNF-R1, p-JNK, caspase-8 and t-Bid detection, 25 μg of protein was subjected to 12% SDS-polyacrylamide gel electrophoresis and transferred to PVDF membranes. For TNF-α detection, 25 μg of protein was subjected

Table 1
Evaluation of induced diabetes and effect of all treatments.

	Control	Control + a-TNF-α	Control + AG	SID	SID + I	SID + AG	SID + a-TNF-α
Blood glucose (mmol/l)	6.5 ± 0.1	6.7 ± 0.4†	5.7 ± 0.2†	25.9 ± 2.3*	4.7 ± 0.1†	25.3 ± 1.2*	23.9 ± 0.2*
Body weight (g)	440 ± 9	432 ± 7†	430 ± 15†	298 ± 9*	421 ± 13†	309 ± 5*	301 ± 5*
ALT (U/l)	11.5 ± 5.5	27.0 ± 1.5†	19.3 ± 2.3†	34.5 ± 2.5*	17.2 ± 3.5†	66.0 ± 1.2*	124.3 ± 3.5*
AST (U/l)	102.0 ± 8.0	104.3 ± 13.0†	91.3 ± 10.4†	204.0 ± 21.7*	101.7 ± 3.1†	251.7 ± 30.0*	194.7 ± 14.9*

Control: vehicle; Control + a-TNF-α: Control treated with etanercept; Control + AG: Control treated with AG SID: Streptozotocin-induced diabetes; SID + I: Streptozotocin-induced diabetes treated with insulin; SID + AG: Streptozotocin-induced diabetes with AG; SID + a-TNF-α: Streptozotocin-induced diabetes with etanercept. Values are mean ± S.E. ($n = 6$ animals per group).

* $p < 0.05$ vs Control.

† $p < 0.05$ vs SID.

to 15% SDS-polyacrylamide gel electrophoresis and transferred to PVDF membranes. After blocking, blots were incubated overnight at 4 °C with either polyclonal anti-iNOS antibody, anti-TNF-α, anti-TNF-R1, anti-p-JNK, anti-caspase-8 (p18) or anti-Bid (1:300, Santa Cruz Biotechnology, Santa Cruz, CA, USA). Membranes were then incubated with either anti-rabbit or anti-mouse Ig G-peroxidase conjugates (1:5000, Amersham Life Science) and the resulting bands were detected by enhanced chemiluminescence detection (ECL; Pierce Western blotting substrate). Autoradiographs were obtained by exposing PVDF membranes to Kodak XAR film and the bands were quantified by densitometry (Shimadzu CS-9000).

2.2.2. NO detection by electron paramagnetic resonance (EPR) spectroscopy

NO production was estimated by EPR spectroscopy. The EPR signal was quantified by detection of triplet of the ternary NO-Fe^{2+}-$(DETC)_2$ complex centered at $g = 3.30$. The vertical amplitude of this triplet signal is proportional to the concentration of bound NO (Henry et al., 1991). Rats from each experimental group, Control, Control + a-TNF-α, Control + AG, SID, SID + I, SID + a-TNF-α and SID + AG were especially treated in accordance with the following protocol: Thirty minutes before euthanasia, all animals were treated with ferrous sulfate (37.5 mg/kg body weight, Cicarelli) and disodium citrate dehydrate (187.5 mg/kg b.w., Cicarelli), sc afterwards, diethyldithiocarbamate (DETC, 500 mg/kg b.w., Anedra), was administered i.p. Animals were anesthetized and euthanatized and livers were promptly removed. After a rapid washing in cold saline solution, samples were placed in 1 ml syringes, frozen and kept in liquid nitrogen until they were subjected to EPR. Samples were transferred to a Dewar and EPR spectra were recorded at liquid nitrogen temperature on a Bruker ECS 106 ESR, operating under the following conditions: 9.41 GHz microwave frequency, 10 mW microwave power, 4.75 G modulation amplitude and 3350 G central field; measurements were performed at RG: 1 × 103 and 1 scan (Mikoyan et al., 1997; Obolenskaya et al., 1994).

2.2.3. NFκB determination

The nuclear factor NFκB p50/p65 heterodimer regulates diverse cellular functions such as immune response and cell growth. The activation of NFκB has been implicated in the transcription regulation of a variety of genes (van den et al., 2001). To investigate heterodimer activity in liver of diabetic rats, p50/p65 EZ-TFA Transcription Factor Assay (Millipore®) was performed according to the manufacturer's instructions. NFκB activity assay was performed by colorimetric determination of p65 subunit in the following experimental groups ($n = 6$): Control, SID, SID + I, Control + a-TNF-α, Control + AG, SID + a-TNF-α and SID + AG. Liver nuclear fractions were obtained by homogenization of frozen tissues in lysis buffer with 1 mM phenylmethylsulfonyl fluoride, 10 μg/ml leupeptin, 1 μg/ml aprotinin and 2% Triton X-100. After centrifugation at 5000 rpm for 5 min, pellet was resuspended in the same lysis buffer but without Triton X-100 and centrifuged to 5000 rpm for other 10 min again. Pellets were resuspended in buffer Hepes 20 mM, NaCl 0.4 M, EDTA 1 mM, EGTA 1 mM, 20% glycerol, protease inhibitor and dTT. Proteins were quantified by Lowry's method (Lowry et al., 1951). P50 activity was measured spectrophotometrically at λ450 nm.

2.2.4. Caspase-8 activity assay

Determination of caspase activities was carried out using a fluorometric assay kit (caspase-8 activity assay kit QIA71; Calbiochem®) according to the manufacturer's instructions. The tissues were homogenized in lysis buffer (10 mM Tris, 200 mM NaCl, 1 mM EDTA, 0.001% Triton X-100). The cytosolic fraction from each sample was obtained by differential centrifugation. After the addition of caspase-8 fluorescent substrate conjugates (10 μl/well) and incubation at 37 °C for 2 h, fluorescence was read in a DTX 880 multimode detector (Beckman Coulter) at an excitation wavelength of 400 nm and an emission wavelength of 405 nm.

2.3. Assessment of apoptotic cell death

Caspase-3 activity and terminal deoxynucleotidyl transferase-mediated dUTP-biotin nick end labeling (TUNEL) assays were performed as quantitative indexes of apoptosis.

2.3.1. Caspase-3 activity assay

The activity of caspase-3 was determined according to the manufacturer's instructions using an EnzChek™ caspase-3 assay kit (Molecular Probes, USA). The tissues were homogenized in lysis buffer (10 mM Tris, 200 mM NaCl, 1 mM EDTA, 0.001% Triton X-100). After differential centrifugation, the cytosolic fraction from each sample was mixed with Z-Asp-Glu-Val-Asp-AMC substrate solution. A standard curve of AMC ranging from 0 to 100 μM was run with each set of samples. A control sample without enzyme was used in each assay to determine the background fluorescence of the substrate. As an additional control, 1 μl of 1 mM Ac-Asp-Glu-Val-Asp-CHO (aldehyde), the caspase-3 inhibitor stock solution, was added. Fluorescence was measured at an excitation wavelength of 360 nm and an emission wavelength of 465 nm in a DTX 880 multimode detector (Beckman Coulter) (Frances et al., 2010).

2.3.2. Determination of apoptotic index (AI)

An apoptosis detection system was utilized which catalytically incorporates fluorescein-12-dUTP at the 30-OH DNA ends using the principle of the TUNEL assay, with direct visualization of the labeled DNA (Promega, Madison, WI, USA). Light microscopic analysis of hematoxylin- and eosin-stained slides was used to quantify apoptotic cells, which were identified by morphological criteria (increased eosinophilic cytoplasm, darkened nucleus, and pycnotic separation of cytoplasmic membrane from neighboring cells). The number of apoptotic hepatocytes by TUNEL and hematoxylin–eosin was assessed by systematically scoring at least 1000 hepatocytes per field in 10 fields of tissue sections at a magnification of 400× (Gold et al., 1994; Klainguti et al., 2000).

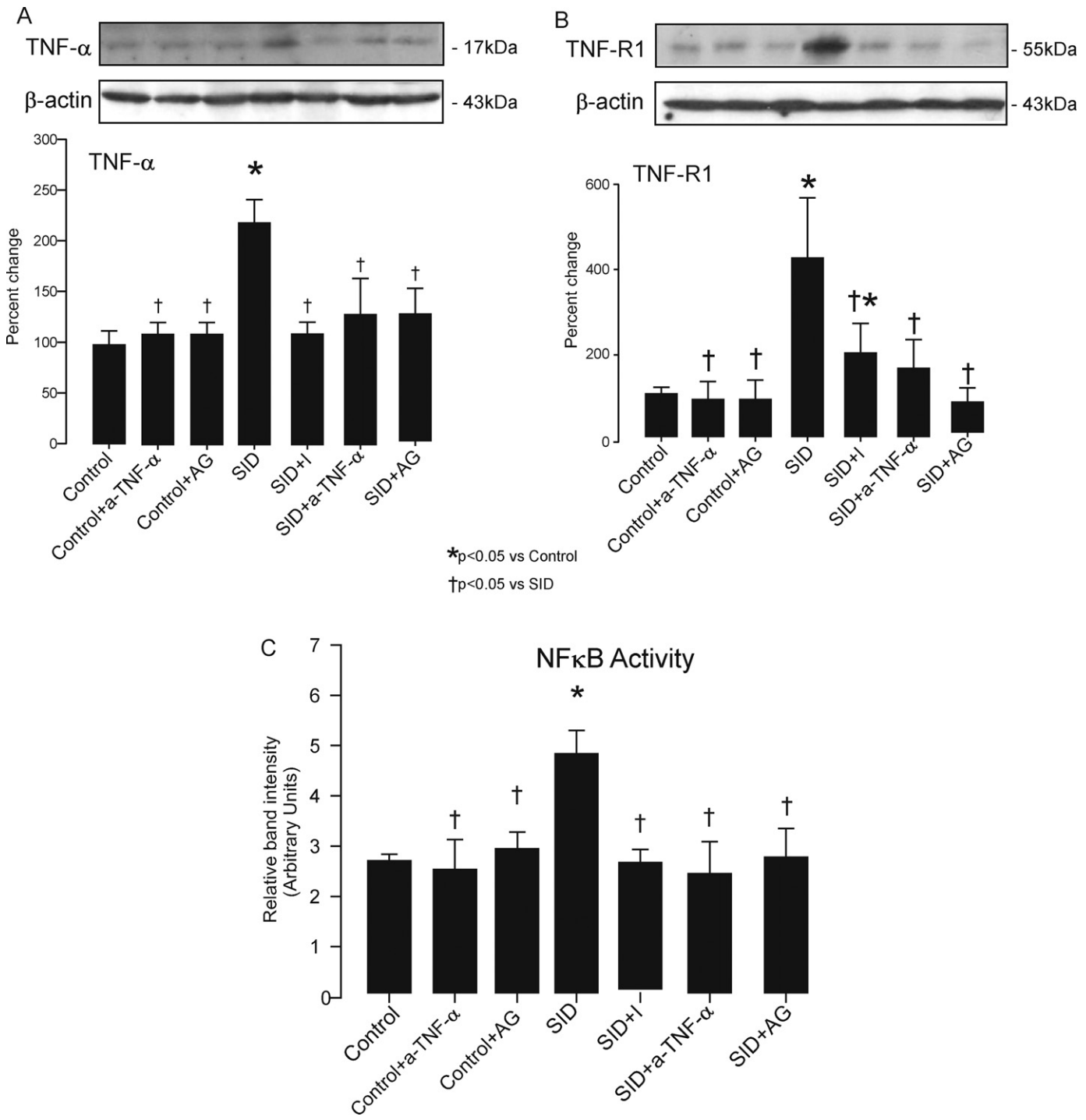

Fig. 1. Hepatic TNF-α and TNF-R1 expression and NFκB activity in STZ-induced diabetic rats. The results obtained for all experimental groups are shown as follows: Lane 1: Control (C): Control group of animals injected with sodium citrate vehicle; lane 2: Control + a-TNF-α: etanercept (8 mg/kg body weight, i.p.) was administered, once a day, twice a week, in saline solution starting 15 days after injection of sodium citrate vehicle and for 15 days; lane 3: Control + AG: aminoguanidine (100 mg/kg body weight, i.p.), was administered, once a day, in saline solution starting 15 days after injection of sodium citrate vehicle and for 3 days before sacrifice; lane 4: SID: streptozotocin (STZ)-induced diabetic rats received an i.p. injection of STZ 60 mg/kg body weight; lane 5: SID + I: on day 15 post-STZ treatment insulin was administered subcutaneously to SID rats twice a day (at 8:00 A.M. and 8:00 P.M.) for 15 days; lane 6: SID + a-TNF-α: etanercept (8 mg/kg body weight, i.p.) was administered, once a day, twice a week, in saline solution starting 15 days after injection of STZ and for 15 days lane 7: SID + AG: aminoguanidine (100 mg/kg body weight, i.p.), was administered, once a day, in saline solution starting 15 days after injection of STZ and for 3 days before sacrifice. Protein immunoblot analysis of TNF-α (A) and TNF-R1 (B) in total liver lysate. Typical examples of Western blots are shown in top panel for each experimental group. The accompanying bars represent the densitometric analysis of the blots as percentage change from six separate animal sets, expressed as arbitrary unit considering control as 100%. Data are expressed as mean ± S.E. (C) NFκB activity is shown as follows: Lane 1: Control; lane 2: Control + a-TNF-α; lane 3: Control + AG; lane 4: SID; lane 5: SID + I; lane 6: SID + a-TNF-α; lane 7: SID + AG. $^{*}p < 0.05$ vs Control; $^{\dagger}p < 0.05$ vs SID.

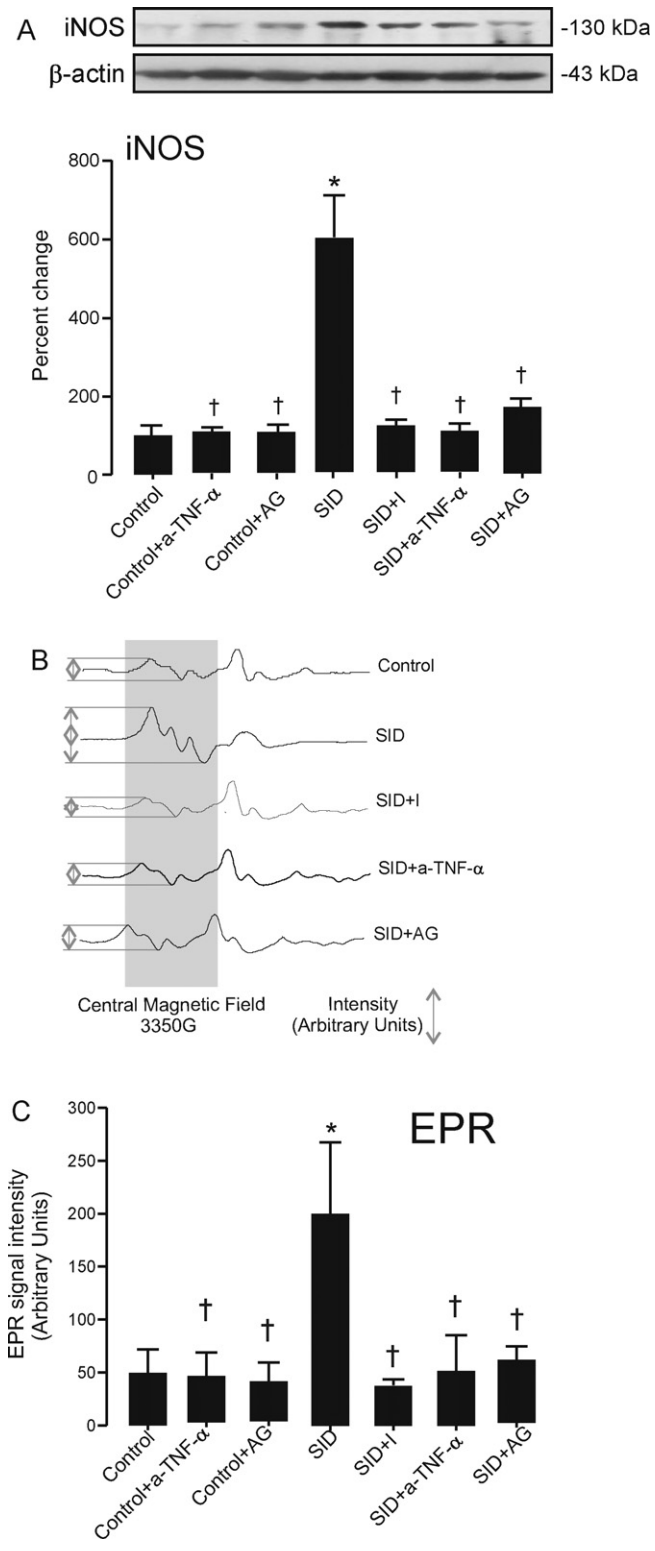

Fig. 2. Panel (A) Immunoblot analysis of iNOS expression in total liver lysate. Effect of the treatments on each experimental group as was described in Fig. 1. Typical examples of Western blots are shown in top panel for each experimental group. The accompanying bars represent the densitometric analysis of the blots expressed as percentage change from six separate animal sets. Data are expressed as mean ± S.E. $^{*}p < 0.05$ vs Control; $^{\dagger}p < 0.05$ vs SID. Panel (B) Representative EPR spectra of NO in liver tissue were recorded at liquid nitrogen temperature on a Bruker ECS 106 ESR, operating at the microwave frequency 9.41 GHz, microwave power 10 mW, modulation amplitude 4.75 G and central field 3350 G and were measured at RG: 1×10^3 and 1 scan. The radical was assessed in the following groups: C, SID and SID + I rats and SID rats pretreated with aminoguanidine and etanercept. Spectra are representative of at least six independent experiments. There are not differences in spectra between C and Control + a-TNF-α or Control + AG (Data not shown). Panel (C) EPR comparative quantization of the effect of different treatments on NO production in diabetic animals: Lane 1: Control; lane 2: Control + a-TNF-α, lane 3: Control + AG, lane 4: SID, lane 5: SID + I, lane 6: SID + a-TNF-α, lane 7: SID + AG. $^{*}p < 0.05$ vs Control; $^{\dagger}p < 0.05$ vs SID.

2.4. Statistical analysis

Data are presented as mean ± S.E. for at least six rats per group. Student's *t*-test was applied wherever necessary, and statistical analysis of differences between groups was performed by one-way ANOVA followed by Tukey's method. Differences were considered as statistically significant when $p < 0.05$.

3. Results

3.1. Evaluation of induced diabetes and effect of all treatments

Diabetes was confirmed in streptozotocin-injected rats by monitoring weight loss and significant increase in blood glucose levels. The status of the serum-specific marker related to hepatic damage is shown in Table 1. We determined serum hepatic enzyme activities by a chemical kit (Wiener Lab, Argentina). According to several authors (Barneo et al., 1990; Fernandes et al., 2010; Hwang et al., 2005; Frances et al., 2010), our results showed that STZ-induced diabetes caused a significant increase in serum ALT (alanine aminotransferase) and AST (aspartate aminotransferase) levels (increased by factors of 3 and 2, respectively). Only, the treatment with insulin could keep these levels close to normal.

As expected, streptozotocin treated rats (SID) showed a significant increase in blood glucose levels and a diminution of body weight (b.w.) (Table 1). Insulin treatment decreased blood glucose levels and increased b.w., reaching the control values. No changes were observed in the parameters tested after treatment of Control and SID groups with etanercept or AG (Table 1).

3.2. Hepatic TNF-α and TNF-R1 expression and NFκB activity in STZ-induced diabetes

Diabetes is considered as an inflammatory disease (Wellen and Hotamisligil, 2005). Thus, we analyzed liver TNF-α and its receptor TNF-R1 levels by Western blot. As shown in Fig. 1A and B, hepatic TNF-α and TNF-R1 levels of the diabetic group were higher than those of the control animals (120% and 300%, respectively). Treatment of SID rats with insulin (SID + I) markedly decreased the hepatic TNF-α levels (reaching the control values) as well as TNF-R1 expression, as expected due to its known anti-inflammatory effect (Fig. 1A and B) (Jeschke et al., 2004). Administration of etanercept or AG also produced a significant attenuation of both TNF-α and TNF-R1 when compared to SID, reaching the control values (Fig. 1A and B).

The diabetic state significantly increased NFκB activity (Fig. 1C) when compared to the Control group ($p < 0.05$), while treatment with insulin significantly attenuated this increment when compared to the SID group (100%, $p < 0.05$) reaching the values of the Control group (Fig. 1C).

3.3. iNOS expression and assessment of NO production in the liver

We examined the expression of iNOS in liver cytosolic fraction by Western blot in all experimental groups. Immunoblot analysis followed by quantitative densitometry from six separate animal sets revealed that iNOS increased by 500% ($p < 0.05$) in SID rats compared to the Control group (Fig. 2A). Treatment of SID rats with insulin or etanercept or AG markedly decreased the

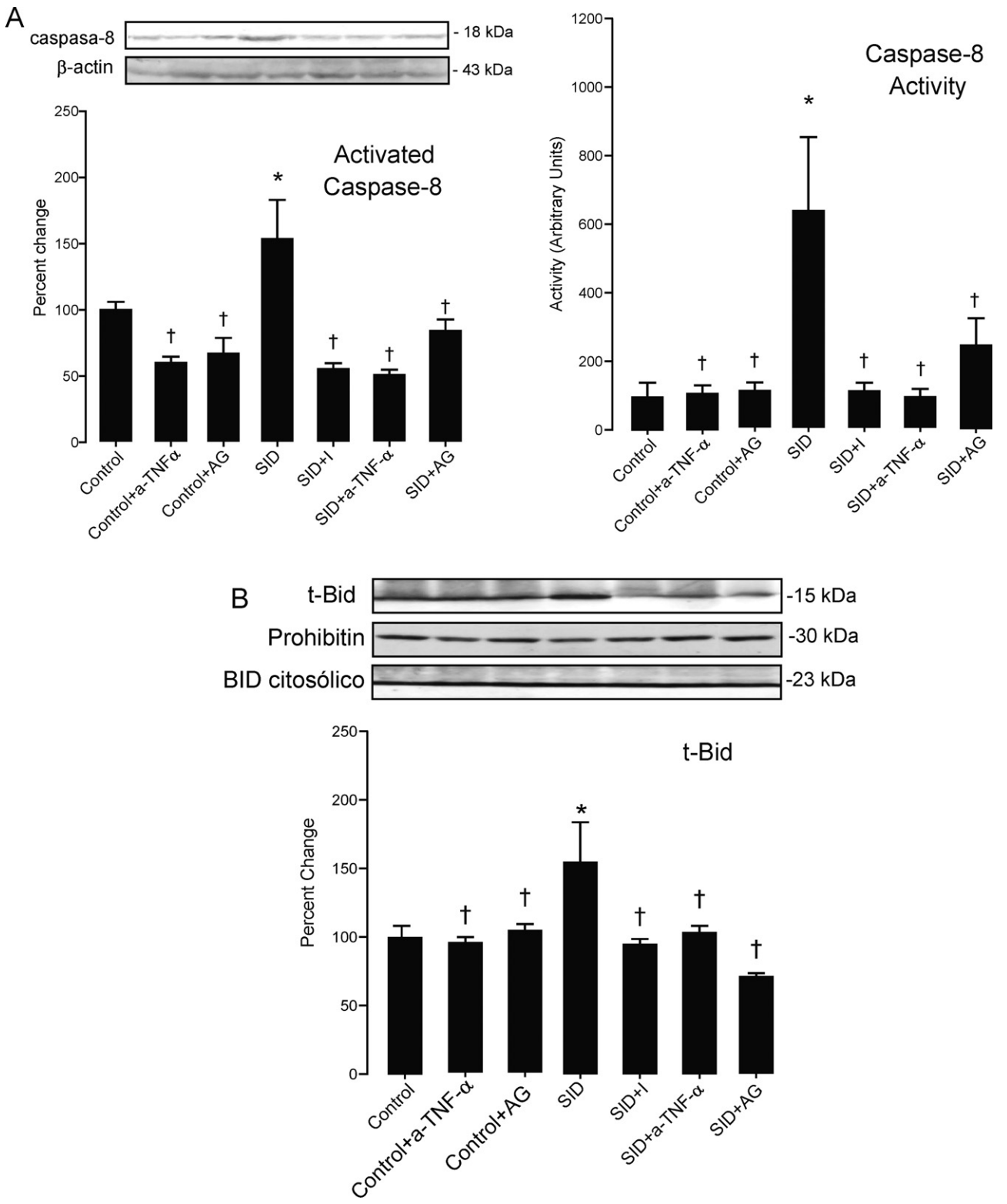

Fig. 3. (A) Activated caspase-8 expression and activity in diabetic liver: protein immunoblot analysis of casapase-8 was performed in cytosol fraction. Caspase-8 activity was determined fluorometrically in cytosol fraction. Activities represented as bars are showed as arbitrary units. Data are expressed as mean ± S.E. for at least six rats for each experimental group. (B) Immunoblotting of cytosolic BID and t-BID expression in mitochondria-enriched fractions of diabetic liver and effect of different treatments in experimental groups as was described in Fig. 1. Typical examples of Western blots are shown for cytosolic BID and mitochondrial t-BID in top panel for each experimental group. The accompanying bars represent the densitometric analysis of the blots for t-BID expressed as percentage change from six separate animal sets. Data are expressed as mean ± S.E. $^{*}p < 0.05$ vs Control; $^{\dagger}p < 0.05$ vs SID.

cytosolic protein levels of iNOS reaching the control values in all cases. The functional iNOS enzyme was confirmed by NO detection. We used in vivo spin-trapping techniques followed by EPR to assess NO production in rat liver. In this assay, the NO reacts with the spin-trapping agent, DETC, producing a stable adduct, NO-Fe^{2+}-$(DETC)_2^-$ which can be detected and characterized through its unique signature EPR spectra. Moreover, the fraction of NO produced can be assessed, thereby allowing comparative quantification (Mikoyan et al., 1997; Obolenskaya et al., 1994). Results are presented in Fig. 2 B and C. The diabetic state increased NO production in liver homogenates (150%) compared with the Control group ($p < 0.05$), and insulin treatment significantly attenuated this increase observed in SID rats ($p < 0.05$ vs SID). A dramatic decrease in the production of NO was found in SID rats when etanercept or AG was administered.

3.4. Determination of activated caspase-8 expression and activity and analysis of t-Bid protein expression in liver

Rats subjected to induction of diabetes by STZ administration exhibited a substantial increase in both expression of activated caspase-8 and their activity in liver cytosolic fraction (Fig. 3A). Insulin treatment resulted in a significant reduction of the caspase-8 activity induced by the diabetic state. This reduction in both activated caspase-8 expression and their activity was not significantly different from the diminution obtained upon administration of etanercept or AG alone.

We also examined the expression of t-Bid in cytosolic fraction and in liver mitochondrial fraction by Western blot in all experimental groups. Inmunoblot analysis followed by quantitative densitometry from six separate animal sets revelated that mitochondrial t-Bid protein levels increased by approximately 50% ($p < 0.05$) in SID group when compared to the Control group (Fig. 3B). Treatment of SID rats with insulin (SID + I) markedly decreased the mitochondrial protein levels of t-Bid, reaching the values of the Control group. Administration of etanercept or AG also produced a significant attenuation of Bid-t in mitochondrial fraction when compared to SID.

3.5. Determination of phosphorylated-JNK (p-JNK)

We evaluated the activation of c-Jun N-terminal kinase (JNK), member of the family of the mitogen-activated protein kinase (MAPK), to assess their potential involvement in the diabetic state. Fig. 4 shows an increase in the amount of p-JNK in the liver of diabetic rats. Insulin treatment decreases the phosphorylation of JNK. In addition, JNK is significantly decreased with the administration of etanercept or AG. The administration of both etanercept and AG prevents the hyperglycemia-induced phosphorylation of JNK.

3.6. Assessment of apoptotic cell death

Caspase-3 activity and TUNEL assays were performed in order to characterize the effect of the diabetic state on induced apoptosis in the liver. Results are presented in Fig. 5. Caspase-3 activity was assayed in liver cytosolic fraction in all experimental groups and is presented in Fig. 5A. There was a significant increase in the caspase-3 activity in SID rats when compared to the Control group ($p < 0.05$). The caspase-3 activity was significantly decreased by insulin treatment when compared to SID rats ($p < 0.05$), while no difference was observed when compared to the Control group. The administration of etanercept or AG to SID rats had a similar significant effect on caspase-3 activity as insulin treatment. Fig. 5B shows apoptotic index (AI) expressed as a percentage. Apoptotic cells were identified in all experimental groups. Typical features of apoptosis, such as cellular shrinking with cytoplasmatic acidophilia condensation and margination of chromatin were corroborated by hematoxylin–eosin staining. The diabetic state significantly increased the AI when compared to the Control group ($p < 0.05$), while treatments with insulin or etanercept or AG significantly attenuated this increment when compared to SID group ($p < 0.05$), reaching the control values (Fig. 5B).

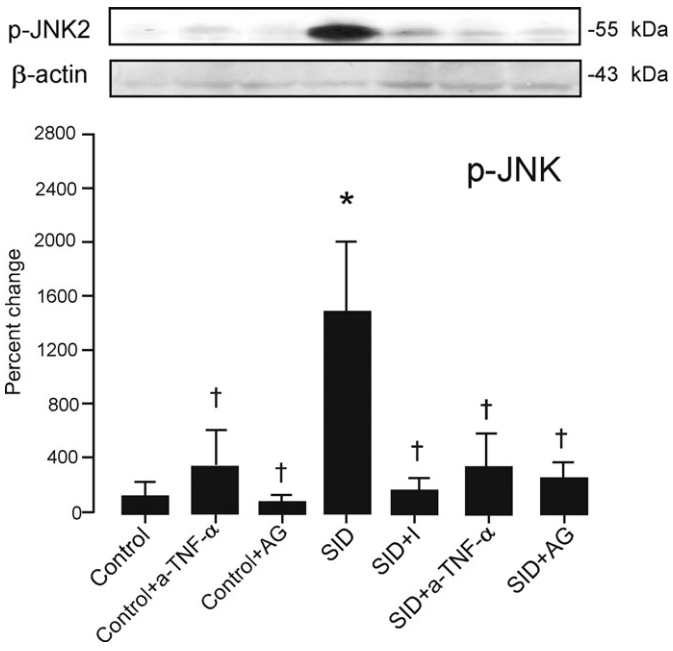

Fig. 4. Western blot analysis of p-JNK in the liver tissue of diabetic animals and effect of different treatments. Typical examples of Western blots are shown in: Lane 1: Control; lane 2: Control + a-TNF-α, lane 3: Control + AG, lane 4: SID, lane 5: SID + I, lane 6: SID + a-TNF-α, lane 7: SID + AG. The accompanying bars represent the densitometric analysis of the blots expressed as percentage from six separate animal sets. Data are expressed as mean ± S.E. $^*p < 0.05$ vs Control; $^\dagger p < 0.05$ vs SID.

In Fig. 5C a representative TUNEL assay for Control, SID, SID + I, Control + etanercept, Control + AG, SID + etanercept and SID + AG is shown. TUNEL-positive signal is maximal in the SID group and it is clear that after the different treatments there is a significant reduction of TUNEL-positive cells. In no case, the careful histological analysis of liver sections stained with hematoxylin–eosin showed inflammatory foci or necrosis (data not shown).

4. Discussion

As diabetes has been considered an inflammatory disease (Wellen and Hotamisligil, 2005), our guiding hypothesis was that TNF-α pathways, through its interaction with TNF-R1, induces caspase-8 and that phosphorylation of JNK could be responsible for the induction of apoptosis in the liver of STZ-induced diabetic rats.

Several studies have shown that TNF-α may be involved in viral hepatitis, alcoholic hepatitis, ischemia/reperfusion liver injury, and fulminant hepatic failure. In human disease, serum levels of plasma TNF-α and hepatic TNF-receptors are frequently increased (Ding and Yin, 2004). Our data demonstrate that the diabetic state induces in the liver an increase of TNF-α and its receptor TNF-R1 (see Fig. 1A and B). NFκB is one of the major transcription factors involved in the unleashing of the cascade of events leading to inflammation, and different research groups have demonstrated its activation in the diabetic liver (Boden et al., 2005; Iwasaki et al., 2007; Bi et al., 2008; Romagnoli et al., 2010). Data presented in Fig. 1 show that the increase of the TNF-α levels in the liver of streptozotocin-induced diabetic rats leads to a marked up-regulation of the NFκB pathway. It is known that NF-κB is involved in many aspects of cell growth,

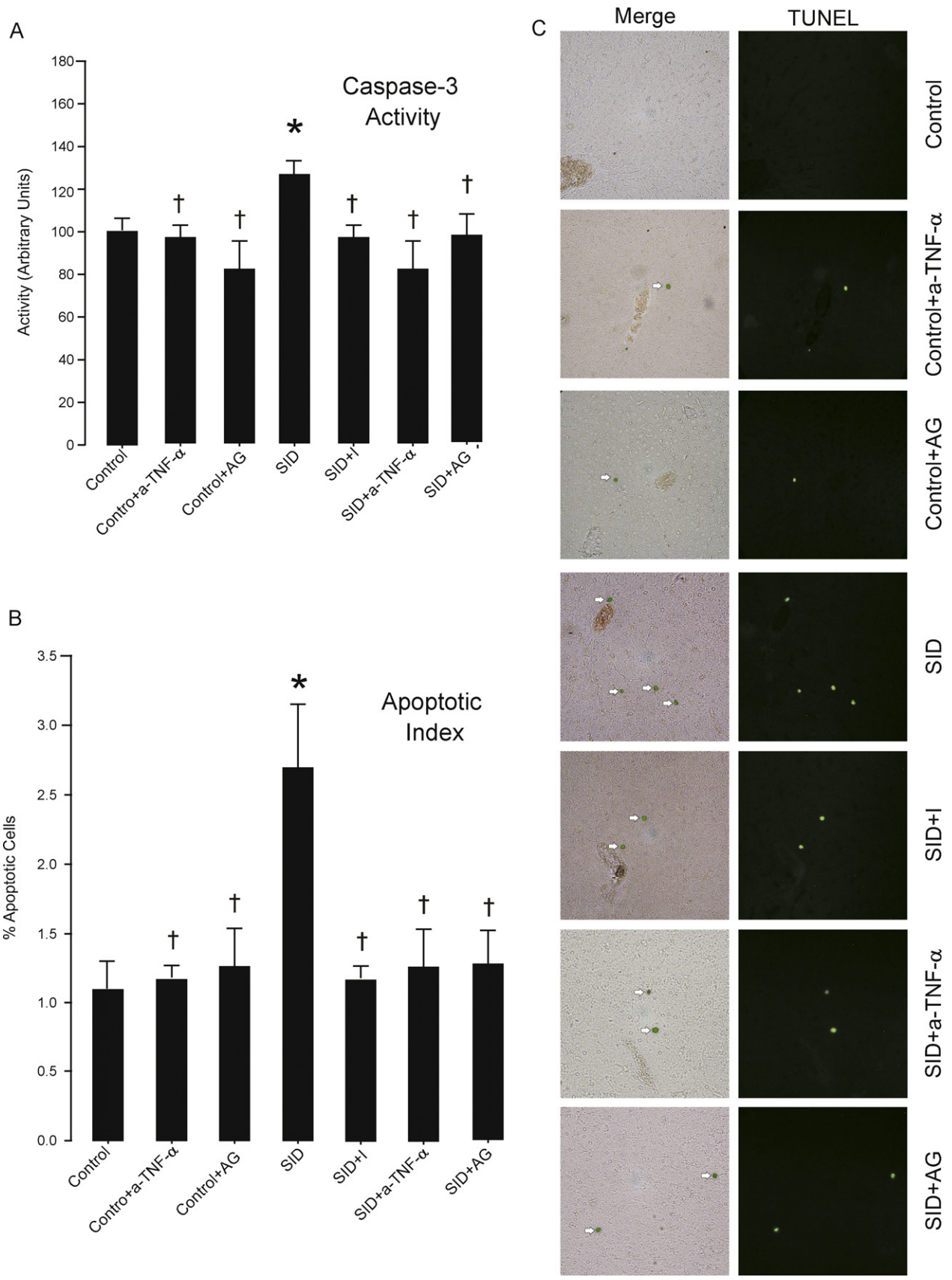

Fig. 5. (A) Caspase-3 activity in diabetic rats and effect of different treatments: The activity of caspase-3 was determined by means of a fluorometric assay. The bars represent activity expressed as arbitrary units. Data are expressed as mean ± S.E. for at least six rats for each experimental group. $^{*}p < 0.05$ vs Control; $^{\dagger}p < 0.05$ vs SID. (B) Effect of NO and TNF-α on liver apoptosis of diabetics rats treated and untreated with insulin: Bars of apoptotic index (AI) represent the percentage of apoptotic cells scored at least 1000 hepatocytes per field in 10 fields of tissue sections at a magnification of 400×. Data are expressed as mean ± S.E. for at least six rats for each experimental group. $^{*}p < 0.05$ vs Control; $^{\dagger}p < 0.05$ vs SID. (C) TUNEL assay: A representative TUNEL assay was performed on liver slides taken from Control, Control + a-TNF-α, Control + AG, SID, SID + I, SID + a-TNF-α and SID + AG groups.

differentiation, proliferation and apoptosis through the regulation of genes by leading to inflammatory, fibrinogenic, and carcinogenic responses (Baldwin, 1996; Dandona et al., 2007; Fujioka et al., 2004; Yang et al., 2011). The expression of iNOS is closely related to the up-regulation of nuclear factor kappa B. NFκB sites have been identified in the promoter region of the iNOS gene (Saccani et al., 2001). The latter was evaluated by the significant rise of iNOS protein level observed in the hepatic tissue of the same animals (see Fig. 2). High levels of TNF-α due to blood glucose levels increased iNOS expression leading to a high production of NO (see Fig. 3). Similar findings have been reported in different tissues by other authors (Stadler et al., 2003; Powell et al., 2004; Madar et al., 2005). Insulin treatment of SID animals is accompanied by marked reductions in iNOS as a result of the decrease of both TNF-α and TNF-R1 expressions, as well as a decline of NFκB activity. The same was reported by other researches working with different tissues (Powell et al., 2004; Begum and Ragolia, 2000). Moreover, Crisafulli et al. and Fries et al. demonstrated that the pharmacological inhibition of TNF-α decreased TNF-R1 and its intracellular signaling (Crisafulli et al., 2009; Fries et al., 2008). In accordance, in our work, the anti-TNF-α treatment of SID rats led to the diminution in the expression of TNF-R1 (Fig. 1B). The diminution of TNF-α level by etanercept-treatment seems to completely abolish the observed increase in iNOS expression induced by the diabetic state. Also, this treatment reduces subsequent production of NO in liver of STZ-induced diabetic rats (Fig. 2). High concentrations of glucose have been shown to increase cytokine-induced increases in iNOS protein (Noh et al., 2002; Xu et al., 1999) in rat tissues. These results are in accordance with our observations, since high blood glucose does not increase iNOS protein in the absence of the cytokine TNF-α. The inhibition of iNOS with a selective inhibitor as aminoguanidine also reduces production of NO in the liver of STZ-induced diabetic rats. iNOS expression together with NO level can be an adequate estimation of enzyme activity (Hickey et al., 2002; Ronco et al., 2007; Zeini et al., 2005). Furthermore, the blockage of iNOS activity decreases TNF-α production. With these results, we clearly demonstrated an interaction between TNF-α pathways and iNOS induction. In addition, our results show that TNF-α is significantly reduced in diabetic rats treated with aminoguanidine. In this connection, Sass et al. demonstrated that iNOS-derived NO regulates pro-inflammatory genes in vivo (Sass et al., 2001).

Importantly, our work shows, for the first time in an in vivo model, an increase of TNF-α which induces the expression of TNF-R1 in the liver of STZ-induced diabetic rats. This augmentation leads to the activation of NFκB and the subsequent activation of iNOS and increased NO production.

Following TNF-α binding to the TNF-R1, an adaptor molecule (TRADD, TNF receptor-associated DD protein), is recruited by the dead domain (DD) to form the first protein complex, which also includes TRAF2 (Erroi et al., 1993). This complex then dissociates from TNF-R1 and forms a different complex in the cytosol, which binds FADD (Fas-associated DD protein), and then recruits caspase-8. Cleavage of pro-caspase 8 allows the release of activated caspase-8 (Cottet et al., 2002). Caspase-8 can cleave Bid to form an active fragment, t-Bid (Zhao et al., 2003). In the liver of STZ-induced diabetic rats we observed an increase in the pathway that begins with the triggering of receptor TNF-R1 by TNF-α, demonstrated by increased expression and activity of caspase-8 and mitochondrial t-Bid (see Fig. 3A and B). Administration of insulin to SID group was shown to cause a significant decrease of activated caspase-8 expression and activity and mitochondrial t-Bid when compared with STZ-induced diabetic rats. According to that described by other authors in different tissues (Crisafulli et al., 2009; Fries et al., 2008) the anti-TNF-α (etanercept) treatment was demonstrated to produce a declination in the response of receptor TNF-R1 to TNF-α (diminished activated caspase-8 expression and activity and mitochondrial protein tBid, in comparison with SID group). Unexpectedly, the treatment with iNOS-inhibitor showed a significant decrease of activated caspase-8 expression and activity in comparison with STZ-induced diabetic rats (Fig. 4A). There are two possible explanations for these observations. One of them is based on the demonstration that NO leads to up-regulation of caspase-8 (Du et al., 2006; Li et al., 2007) thus we propose that a diminution of NO production may be associated with the observed decrease of caspase-8 activity. The second possibility is based on the demonstration that the amount of plasma TNF-α and intrahepatic TNF-α mRNA and protein levels are significantly reduced in iNOS knockout mice (Sass et al., 2001), leading to a decreased activation of caspase-8. Consistent with this, we propose that the treatment with specific iNOS inhibitor aminoguanidine may be associated with the decrease of activated caspase-8 expression and activity observed.

As outlined earlier, the binding of TNF-α to TNF-R1 ultimately leads to the activation of caspase-8 (Wajant, 2003; Micheau and Tschopp, 2003). Activated casapase-8 initiates a proteolytic cascade that results in cleavage of the pro-apoptotic protein Bid (Yin, 2000), initiation of the mitochondrial death pathway with release of cytochrome *c*, and activation of effectors caspase-3 that ultimately induce apoptosis (Zhao et al., 2001). Our results clearly show that in the liver of STZ-induced diabetic rats there is an enlargement of caspase-3 activity with the consequent increase in the AI (Fig. 5). In addition, the hormone treatment showed a significant diminution of AI, reaching the control values due to a normal caspase-3 activity (Fig. 5). A large body of evidence has shown the mediation by PI3K and Akt in the anti-apoptotic action of insulin in a variety of cell types (Lawlor and Alessi, 2001; Xi et al., 2005; Ricci et al., 2008). In this work, data strongly suggest that insulin, also, exerts anti-apoptotic actions in the liver through a diminution of TNF-α-induced death receptor pathway (Figs. 1 and 4) may be due to its anti-inflammatory property as has been described previously (Jeschke et al., 2008). As expected, the anti-TNF-α (etanercept) treatment showed a reduction of the cascade of events leading to apoptotic cell death (Figs. 4 and 5). Etanercept treatment showed a significant diminution of AI, reaching the control values due to a normal caspase-3 activity (Fig. 5). In addition, AG-treatment (which showed a diminution of TNF-α level) decreases caspase-8 and caspase-3 activities, resulting in effective blockade of apoptosis in the liver of STZ-diabetic rats (Fig. 5).

The marked increase in the activity of caspase-8 and NO levels compared with a slight increase in the activity of caspase-3 and the apoptotic index observed in the liver of STZ-diabetic rats could be explained by the complex regulation of the mediators involved in triggering apoptosis. In this sense, apoptosis could proceed along the extrinsic pathway (death receptor pathway) or the intrinsic pathway (mitochondrial pathway), which interacts with each other broadly (Chen et al., 2007). The need for the mitochondrial pathway in the activation and progression of death receptor-mediated apoptosis varies considerably, depending on the type of cells, the type of stimuli, and the strength of the stimulation. In a previous work, we have demonstrated that diabetes induces liver apoptosis via mitochondrial pathway through the increases of hydroxyl radical (Frances et al., 2010).

An early study had demonstrated that the activation of JNK is associated with increased TNF-induced apoptosis hepatocytes (Wullaert et al., 2006). In this connection, our results demonstrate that the diabetes leads to the activation of JNK, inducing an increase of the apoptotic index. Moreover, we demonstrated that the diminution of TNF-α levels by the treatment with etanercept seems to completely abolish the observed activation of JNK induced by the diabetic state, leading to the diminution of the apoptosis (Figs. 4 and 5).

Overall, in the present study we demonstrated that in the diabetes enhances TNF-α in the liver, which may be a fundamental

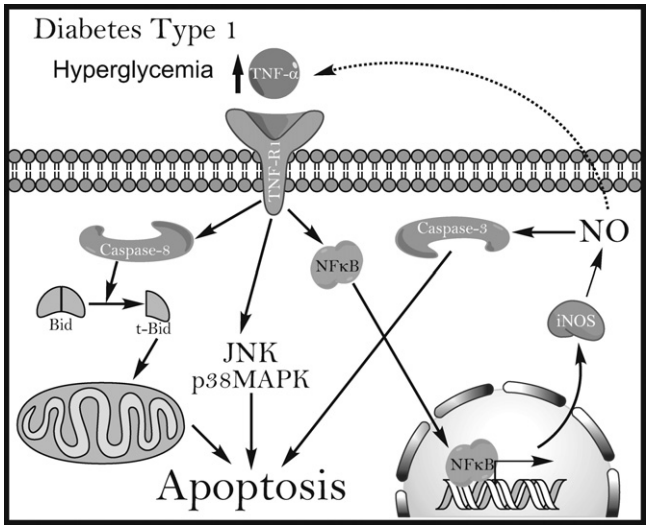

Fig. 6. Proposed scheme for mechanism involved in the TNF-α-induced apoptosis in diabetes type 1 liver disease. In diabetic state the hepatic TNF-α elevation induces activation of NFκB, caspase-8 and JNK, which leads to an increase in apoptotic event.

key leading to apoptotic cell death, through activation of caspase-8, NFκB and JNK pathways (Fig. 6). The relevance of our study is to provide further knowledge about the mechanisms which may contribute to the liver complications associated with type 1 diabetes. The regulation of hepatic TNF-α level and iNOS activity in the diabetic state could be of therapeutic relevance for improvement or delay of the hepatic complications linked to chronic hyperglycemia.

Acknowledgments

This work was supported by research grants from ANPCyT (PICT No. 32413, Cristina E. Carnovale) and from CONICET (PIP No. 5531, Cristina E. Carnovale). We especially wish to thank Dr Cecilia Basiglio for language revision.

References

Alexandraki, K.I., Piperi, C., Ziakas, P.D., Apostolopoulos, N.V., Makrilakis, K., Syriou, V., amanti-Kandarakis, E., Kaltsas, G., Kalofoutis, A., 2008. Cytokine secretion in long-standing diabetes mellitus type 1 and 2: associations with low-grade systemic inflammation. J. Clin. Immunol. 28, 314–321.

Baldwin Jr., A.S., 1996. The NF-kappa B and I kappa B proteins: new discoveries and insights. Annu. Rev. Immunol. 14, 649–683.

Barneo, L., Esteban, M.M., Garcia-Pravia, C., Diaz, F., Marin, B., 1990. Normalization of the altered liver function tests after islet transplantation in diabetic rats. Diabetes Metab. 16, 284–289.

Begum, N., Ragolia, L., 2000. High glucose and insulin inhibit VSMC MKP-1 expression by blocking iNOS via p38 MAPK activation. Am. J. Physiol. Cell Physiol. 278, C81–C91.

Bi, Y., Sun, W.P., Chen, X., Li, M., Liang, H., Cai, M.Y., Zhu, Y.H., He, X.Y., Xu, F., Weng, J.P., 2008. Effect of early insulin therapy on nuclear factor kappaB and cytokine gene expressions in the liver and skeletal muscle of high-fat diet, streptozotocin-treated diabetic rats. Acta Diabetol. 45, 167–178.

Boden, G., She, P., Mozzoli, M., Cheung, P., Gumireddy, K., Reddy, P., Xiang, X., Luo, Z., Ruderman, N., 2005. Free fatty acids produce insulin resistance and activate the proinflammatory nuclear factor-kappaB pathway in rat liver. Diabetes 54, 3458–3465.

Brune, B., von, K.A., Sandau, K.B., 1999. Nitric oxide (NO): an effector of apoptosis. Cell Death Differ. 6, 969–975.

Budihardjo, I., Oliver, H., Lutter, M., Luo, X., Wang, X., 1999. Biochemical pathways of caspase activation during apoptosis. Annu. Rev. Cell Dev. Biol. 15, 269–290.

Carnovale, C.E., Marinelli, R.A., Rodriguez Garay, E.A., 1986. Bile flow decrease and altered bile composition in streptozotocin-treated rats. Biochem. Pharmacol. 35, 2625–2628.

Carnovale, C.E., Rodriguez Garay, E.A., 1984. Reversible impairment of hepatobiliary function induced by streptozotocin in the rat. Experientia 40, 248–250.

Carnovale, C.E., Scapini, C., Alvarez, M.L., Favre, C., Monti, J., Carrillo, M.C., 2000. Nitric oxide release and enhancement of lipid peroxidation in regenerating rat liver. J. Hepatol. 32, 798–804.

Chen, X., Ding, W.X., Ni, H.M., Gao, W., Shi, Y.H., Gambotto, A.A., Fan, J., Beg, A.A., Yin, X.M., 2007. Bid-independent mitochondrial activation in tumor necrosis factor alpha-induced apoptosis and liver injury. Mol. Cell Biol. 27, 541–553.

Cottet, S., Dupraz, P., Hamburger, F., Dolci, W., Jaquet, M., Thorens, B., 2002. cFLIP protein prevents tumor necrosis factor-alpha-mediated induction of caspase-8-dependent apoptosis in insulin-secreting betaTc-Tet cells. Diabetes 51, 1805–1814.

Crisafulli, C., Galuppo, M., Cuzzocrea, S., 2009. Effects of genetic and pharmacological inhibition of TNF-alpha in the regulation of inflammation in macrophages. Pharmacol. Res. 60, 332–340.

Dandona, P., Chaudhuri, A., Ghanim, H., Mohanty, P., 2007. Proinflammatory effects of glucose and anti-inflammatory effect of insulin: relevance to cardiovascular disease. Am. J. Cardiol. 99, 15B–26B.

Davis, K.L., Martin, E., Turko, I.V., Murad, F., 2001. Novel effects of nitric oxide. Annu. Rev. Pharmacol. Toxicol. 41, 203–236.

Ding, W.X., Yin, X.M., 2004. Dissection of the multiple mechanisms of TNF-alpha-induced apoptosis in liver injury. J. Cell Mol. Med. 8, 445–454.

Du, C., Guan, Q., Diao, H., Yin, Z., Jevnikar, A.M., 2006. Nitric oxide induces apoptosis in renal tubular epithelial cells through activation of caspase-8. Am. J. Physiol. Renal Physiol. 290, F1044–F1054.

Erroi, A., Fantuzzi, G., Mengozzi, M., Sironi, M., Orencole, S.F., Clark, B.D., Dinarello, C.A., Isetta, A., Gnocchi, P., Giovarelli, M., 1993. Differential regulation of cytokine production in lipopolysaccharide tolerance in mice. Infect. Immun. 61, 4356–4359.

Esposito, K., Nappo, F., Marfella, R., Giugliano, G., Giugliano, F., Ciotola, M., Quagliaro, L., Ceriello, A., Giugliano, D., 2002. Inflammatory cytokine concentrations are acutely increased by hyperglycemia in humans: role of oxidative stress. Circulation 106, 2067–2072.

Fernandes, A.A., Novelli, E.L., Okoshi, K., Okoshi, M.P., Di Muzio, B.P., Guimaraes, J.F., Fernandes, J.A., 2010. Influence of rutin treatment on biochemical alterations in experimental diabetes. Biomed. Pharmacother. 64, 214–219.

Foss, N.T., Foss-Freitas, M.C., Ferreira, M.A., Cardili, R.N., Barbosa, C.M., Foss, M.C., 2007. Impaired cytokine production by peripheral blood mononuclear cells in type 1 diabetic patients. Diabetes Metab. 33, 439–443.

Frances, D., Ronco, M., Monti, J., Ingaramo, P., Pisani, G., Parody, J., Pellegrino, J., Martin-Sanz, P., Carrillo, M., Carnovale, C., 2010. Hyperglycemia induces apoptosis in rat liver through the increase of hydroxyl radical: new insights into the insulin effect. J. Endocrinol. 205, 187–200.

Fries, W., Muja, C., Crisafulli, C., Costantino, G., Longo, G., Cuzzocrea, S., Mazzon, E., 2008. Infliximab and etanercept are equally effective in reducing enterocyte APOPTOSIS in experimental colitis. Int. J. Med. Sci. 5, 169–180.

Fujioka, S., Schmidt, C., Sclabas, G.M., Li, Z., Pelicano, H., Peng, B., Yao, A., Niu, J., Zhang, W., Evans, D.B., Abbruzzese, J.L., Huang, P., Chiao, P.J., 2004. Stabilization of p53 is a novel mechanism for proapoptotic function of NF-kappaB. J. Biol. Chem. 279, 27549–27559.

Gold, R., Schmied, M., Giegerich, G., Breitschopf, H., Hartung, H.P., Toyka, K.V., Lassmann, H., 1994. Differentiation between cellular apoptosis and necrosis by the combined use of in situ tailing and nick translation techniques. Lab. Invest. 71, 219–225.

Haidara, M.A., Mikhailidis, D.P., Rateb, M.A., Ahmed, Z.A., Yassin, H.Z., Ibrahim, I.M., Rashed, L.A., 2009. Evaluation of the effect of oxidative stress and vitamin E supplementation on renal function in rats with streptozotocin-induced type 1 diabetes. J. Diabetes Complications 23, 130–136.

Harrison, S.A., 2006. Liver disease in patients with diabetes mellitus. J. Clin. Gastroenterol. 40, 68–76.

Henry, Y., Ducrocq, C., Drapier, J.C., Servent, D., Pellat, C., Guissani, A., 1991. Nitric oxide, a biological effector. Electron paramagnetic resonance detection of nitrosyl-iron-protein complexes in whole cells. Eur. Biophys. J. 20, 1–15.

Hickey, M.J., Sihota, E., Amrani, A., Santamaria, P., Zbytnuik, L.D., Ng, E.S., Ho, W., Sharkey, K.A., Kubes, P., 2002. Inducible nitric oxide synthase (iNOS) in endotoxemia: chimeric mice reveal different cellular sources in various tissues. FASEB J. 16, 1141–1143.

Ho, F.M., Lin, W.W., Chen, B.C., Chao, C.M., Yang, C.R., Lin, L.Y., Lai, C.C., Liu, S.H., Liau, C.S., 2006. High glucose-induced apoptosis in human vascular endothelial cells is mediated through NF-kappaB and c-Jun NH2-terminal kinase pathway and prevented by PI3K/Akt/eNOS pathway. Cell Signal. 18, 391–399.

Hwang, S.L., Liu, I.M., Tzeng, T.F., Cheng, J.T., 2005. Activation of imidazoline receptors in adrenal gland to lower plasma glucose in streptozotocin-induced diabetic rats. Diabetologia 48, 767–775.

Iwasaki, Y., Kambayashi, M., Asai, M., Yoshida, M., Nigawara, T., Hashimoto, K., 2007. High glucose alone, as well as in combination with proinflammatory cytokines, stimulates nuclear factor kappa-B-mediated transcription in hepatocytes in vitro. J. Diabetes Complications 21, 56–62.

Jeschke, M.G., Klein, D., Bolder, U., Einspanier, R., 2004. Insulin attenuates the systemic inflammatory response in endotoxemic rats. Endocrinology 145, 4084–4093.

Jeschke, M.G., Klein, D., Thasler, W.E., Bolder, U., Schlitt, H.J., Jauch, K.W., Weiss, T.S., 2008. Insulin decreases inflammatory signal transcription factor expression in primary human liver cells after LPS challenge. Mol. Med. 14, 11–19.

Kim, J.Y., Lee, S.H., Song, E.H., Park, Y.M., Lim, J.Y., Kim, D.J., Choi, K.H., Park, S.I., Gao, B., Kim, W.H., 2009. A critical role of STAT1 in streptozotocin-induced diabetic liver injury in mice: controlled by ATF3. Cell Signal. 21, 1758–1767.

Klainguti, M., Aigner, S., Kilo, J., Eppenberger, H.M., Mandinova, A., Aebi, U., Schaub, M.C., Shaw, S.G., Luscher, T.F., Atar, D., 2000. Lack of nuclear apoptosis in cardiomyocytes and increased endothelin-1 levels in a rat heart model of myocardial stunning. Basic Res. Cardiol. 95, 308–315.

Kolb, J.P., 2000. Mechanisms involved in the pro- and anti-apoptotic role of NO in human leukemia. Leukemia 14, 1685–1694.
Kruidering, M., Evan, G.I., 2000. Caspase-8 in apoptosis: the beginning of "the end"? IUBMB. Life 50, 85–90.
Lawlor, M.A., Alessi, D.R., 2001. PKB/Akt: a key mediator of cell proliferation, survival and insulin responses? J. Cell Sci. 114, 2903–2910.
Li, L., Zhang, J., Jin, B., Block, E.R., Patel, J.M., 2007. Nitric oxide upregulation of caspase-8 mRNA expression in lung endothelial cells: role of JAK2/STAT-1 signaling. Mol. Cell Biochem. 305, 71–77.
Lowry, O.H., Rosebrough, N.J., Farr, A.L., Randall, R.J., 1951. Protein measurement with the Folin phenol reagent. J. Biol. Chem. 193, 265–275.
Madar, Z., Kalet-Litman, S., Stark, A.H., 2005. Inducible nitric oxide synthase activity and expression in liver and hepatocytes of diabetic rats. Pharmacology 73, 106–112.
Madhusudan, S., Muthuramalingam, S.R., Braybrooke, J.P., Wilner, S., Kaur, K., Han, C., Hoare, S., Balkwill, F., Ganesan, T.S., 2005. Study of etanercept, a tumor necrosis factor-alpha inhibitor, in recurrent ovarian cancer. J. Clin. Oncol. 23, 5950–5959.
Martin-Sanz, P., Hortelano, S., Callejas, N.A., Goren, N., Casado, M., Zeini, M., Bosca, L., 2002. Nitric oxide in liver inflammation and regeneration. Metab. Brain Dis. 17, 325–334.
Micheau, O., Tschopp, J., 2003. Induction of TNF receptor I-mediated apoptosis via two sequential signaling complexes. Cell 114, 181–190.
Mikoyan, V.D., Kubrina, L.N., Serezhenkov, V.A., Stukan, R.A., Vanin, A.F., 1997. Complexes of Fe^{2+} with diethyldithiocarbamate or N-methyl-D-glucamine dithiocarbamate as traps of nitric oxide in animal tissues: comparative investigations. Biochim. Biophys. Acta 1336, 225–234.
Noh, H., Ha, H., Yu, M.R., Kang, S.W., Choi, K.H., Han, D.S., Lee, H.Y., 2002. High glucose increases inducible NO production in cultured rat mesangial cells. Possible role in fibronectin production. Nephron 90, 78–85.
Obolenskaya, M.Y., Vanin, A.F., Mordvintcev, P.I., Mulsch, A., Decker, K., 1994. EPR evidence of nitric oxide production by the regenerating rat liver. Biochem. Biophys. Res. Commun. 202, 571–576.
Powell, L.A., Warpeha, K.M., Xu, W., Walker, B., Trimble, E.R., 2004. High glucose decreases intracellular glutathione concentrations and upregulates inducible nitric oxide synthase gene expression in intestinal epithelial cells. J. Mol. Endocrinol. 33, 797–803.
Rabkin, S.W., Klassen, S.S., 2007. Nitric oxide differentially regulates the gene expression of caspase genes but not some autophagic genes. Nitric Oxide 16, 339–347.
Ricci, C., Jong, C.J., Schaffer, S.W., 2008. Proapoptotic and antiapoptotic effects of hyperglycemia: role of insulin signaling. Can. J. Physiol. Pharmacol. 86, 166–172.
Romagnoli, M., Gomez-Cabrera, M.C., Perrelli, M.G., Biasi, F., Pallardo, F.V., Sastre, J., Poli, G., Vina, J., 2010. Xanthine oxidase-induced oxidative stress causes activation of NF-kappaB and inflammation in the liver of type I diabetic rats. Free Radic. Biol. Med. 49, 171–177.
Ronco, M.T., Alvarez, M.L., Monti, J.A., Carrillo, M.C., Pisani, G.B., Lugano, M.C., Carnovale, C.E., 2004. Role of nitric oxide increase on induced programmed cell death during early stages of rat liver regeneration. Biochim. Biophys. Acta 1690, 70–76.
Ronco, M.T., Frances, D., de Lujan, A.M., Quiroga, A., Monti, J., Parody, J.P., Pisani, G., Carrillo, M.C., Carnovale, C.E., 2007. Vascular endothelial growth factor and nitric oxide in rat liver regeneration. Life Sci. 81, 750–755.
Rosa, S.C., Judas, F., Lopes, M.C., Mendes, A.F., 2008. Nitric oxide synthase isoforms and NF-kappaB activity in normal and osteoarthritic human chondrocytes: regulation by inducible nitric oxide. Nitric Oxide 19, 276–283.
Saccani, S., Pantano, S., Natoli, G., 2001. Two waves of nuclear factor kappaB recruitment to target promoters. J. Exp. Med. 193, 1351–1359.
Sass, G., Koerber, K., Bang, R., Guehring, H., Tiegs, G., 2001. Inducible nitric oxide synthase is critical for immune-mediated liver injury in mice. J. Clin. Invest. 107, 439–447.
Stadler, K., Jenei, V., von, B.G., Somogyi, A., Jakus, J., 2003. Increased nitric oxide levels as an early sign of premature aging in diabetes. Free Radic. Biol. Med. 35, 1240–1251.
Stichtenoth, D.O., Frolich, J.C., 1998. Nitric oxide and inflammatory joint diseases. Br. J. Rheumatol. 37, 246–257.
Stockklauser-Farber, K., Ballhausen, T., Laufer, A., Rosen, P., 2000. Influence of diabetes on cardiac nitric oxide synthase expression and activity. Biochim. Biophys. Acta 1535, 10–20.
Traub, O., Van, B.R., 1995. Role of nitric oxide in insulin-dependent diabetes mellitus-related vascular complications. West J. Med. 162, 439–445.
van den, B.R., Haenen, G.R., van den, B.H., Bast, A., 2001. Transcription factor NF-kappaB as a potential biomarker for oxidative stress. Br. J. Nutr. 86 (Suppl. 1), S121–S127.
Wajant, H., 2003. Death receptors. Essays Biochem. 39, 53–71.
Wellen, K.E., Hotamisligil, G.S., 2005. Inflammation, stress, and diabetes. J. Clin. Invest. 115, 1111–1119.
Wullaert, A., Heyninck, K., Beyaert, R., 2006. Mechanisms of crosstalk between TNF-induced NF-kappaB and JNK activation in hepatocytes. Biochem. Pharmacol. 72, 1090–1101.
Xi, W., Satoh, H., Kase, H., Suzuki, K., Hattori, Y., 2005. Stimulated HSP90 binding to eNOS and activation of the PI3-Akt pathway contribute to globular adiponectin-induced NO production: vasorelaxation in response to globular adiponectin. Biochem. Biophys. Res. Commun. 332, 200–205.
Xu, R., Morales, J.A., Muniyappa, R., Skafar, D.F., Ram, J.L., Sowers, J.R., 1999. Interleukin-1beta-induced nitric oxide production in rat aortic endothelial cells: inhibition by estradiol in normal and high glucose cultures. Life Sci. 64, 2451–2462.
Yang, G., Xiao, X., Rosen, D., Cheng, X., Wu, X., Chang, B., Liu, G., Xue, F., Mercado-Uribe, I., Chiao, P.J., Du, X., Liu, J., 2011. The biphasic role of NF-{kappa}B in tumor progression and chemoresistance of ovarian cancer. Clin. Cancer Res., doi:10.1158/1078-0432.CCR-10-3265.
Yin, X.M., 2000. Bid, a critical mediator for apoptosis induced by the activation of Fas/TNF-R1 death receptors in hepatocytes. J. Mol. Med. 78, 203–211.
Zeini, M., Hortelano, S., Traves, P.G., Gomez-Valades, A.G., Pujol, A., Perales, J.C., Bartrons, R., Bosca, L., 2005. Assessment of a dual regulatory role for NO in liver regeneration after partial hepatectomy: protection against apoptosis and retardation of hepatocyte proliferation. FASEB J. 19, 995–997.
Zhao, Y., Ding, W.X., Qian, T., Watkins, S., Lemasters, J.J., Yin, X.M., 2003. Bid activates multiple mitochondrial apoptotic mechanisms in primary hepatocytes after death receptor engagement. Gastroenterology 125, 854–867.
Zhao, Y., Li, S., Childs, E.E., Kuharsky, D.K., Yin, X.M., 2001. Activation of pro-death Bcl-2 family proteins and mitochondria apoptosis pathway in tumor necrosis factor-alpha-induced liver injury. J. Biol. Chem. 276, 27432–27440.